Materials Chemistry and Physics 296 (2023) 127214

Contents lists available at ScienceDirect

Materials Chemistry and Physics

journal homepage: www.elsevier.com/locate/matchemphys

Effect of Ti as co-sputtering target on microstructure and mechanical properties of FeCoNi(CuAl)$_{0.2}$ high-entropy alloy thin films

J.N. Wen [a,1], R.J. Wu [b,1], Y.H. Mi [a], N. Zhang [a], Z.H. Lin [a], S.C. chen [a], Y.Q. Li [a], S.F. Yang [c,*]

[a] School of Materials Science and Engineering, Nanjing Institute of Technology, Nanjing, China
[b] School of Mechanical Engineering, City College of Huizhou, China
[c] School of Mechanical Engineering, Tianjin University of Technology and Education, Tianjin, China

HIGHLIGHTS

- Three types of FeCoNi(CuAl)$_{0.2}$ high entropy alloy films were prepared using different sputtering processes.
- The introduction of Ti reduced the crystallinity of the alloy and caused changes in the phase structure from FCC to BCC.
- These results indicated that the Ti solution caused significant lattice distortion and solution strengthening.

ARTICLE INFO

Keywords:
High entropy alloy films
Sputtering
Microstructure
Indentation and hardness

ABSTRACT

Three different FeCoNi(CuAl)$_{0.2}$ alloy films sputtered with Ti were prepared using magnetron sputtering: single sputtering films of FeCoNi(CuAl)$_{0.2}$ target, co-sputtering films of FeCoNi(CuAl)$_{0.2}$/Ti targets, and alternating sputtering composite films of FeCoNi(CuAl)$_{0.2}$/Ti targets. SEM, XRD, AFM and nano indentation analysis showed that with the increase in Ti content and change in sputtering mode, the main phase structure of the film changed from FCC to BCC. The hardness and elastic modulus of FeCoNi(CuAl)$_{0.2}$/Ti target co-sputtered films reached 7.33 GPa and 145 GPa, respectively. This can be attributed to the large atomic radius of Ti dissolved in the FeCoNi(CuAl)$_{0.2}$ system that caused phase transformation and significant lattice distortion.

1. Introduction

Multi-principal elemental alloys, known as high-entropy alloys display unique properties. Their complexity leads to different effects including high entropy, hysteresis diffusion, lattice distortion, and cocktail effect [1,2]. These four core effects not only result in simple cubic structures of the complex intermetallic compounds, but also provide excellent properties including high strength, high hardness, wear resistance, corrosion resistance, and high temperature stability, among others [3–5]. The remarkable strength and hardness of high entropy alloys result from the lattice distortion caused by differences in the atomic size of the elements (δ) present in the solid solution. Herein, solid solution strengthening depends on atomic size differences [6,10,11].

This study focused on the effects of different sputtering modes and titanium elements on the phase structure and mechanical properties of the film. The effects of Ti on phase change, lattice distortion, strength, and hardness of the films were investigated.

2. Experimental procedure

High entropy alloy target and titanium target with $\varnothing$ 60 × 3 mm were prepared using powder vacuum hot pressing. In these experiments, Si (100) was selected as substrate for film growth. Also, magnetron sputtering (MSP-300B) was selected to prepare three kinds of films: (a) single sputtering films of FeCoNi(CuAl)$_{0.2}$ target; (b) co-sputtering films of FeCoNi(CuAl)$_{0.2}$/Ti targets; and (c) alternating sputtering composite film FeCoNi(CuAl)$_{0.2}$/Ti targets (Table 1). The detailed microstructures were characterized using x-ray diffraction (XRD) and scanning electron microscope (SEM) equipped with energy-dispersive spectrum (EDS). The surface roughness of the film was measured by atomic force microscope (AFM)with a conical tip [9]. Hardness measurements were performed using MH5L nano indentation equipment at room

* Corresponding author.
E-mail address: yangshf@njit.edu.cn (S.F. Yang).
[1] J.N Wen and R.J Wu have contributed equally to this work.

https://doi.org/10.1016/j.matchemphys.2022.127214
Received 1 July 2022; Received in revised form 16 November 2022; Accepted 16 December 2022
Available online 20 December 2022
0254-0584/

Table 1
Experimental parameters used in different magnetron sputtering processes.

	Time	Temperature	Gas flow	Power (Target 2 and target 3)	
Single sputtering	1800s × 4	500 °C	50sccm	–	280W
Co-sputtering	1800s × 4	500 °C	50sccm	30W	280W
Alternate-sputtering	1200s × 6	500 °C	50sccm	30W	280W

temperature.

3. Results and discussion

Fig. 1 shows the XRD patterns of the three samples. Data indicated that single sputtering films were composed of simple FCC solid solution similar to the Fe–Ni solid solution (PDF#: 47–1405). However, when the sputtering mode varied, as Ti was introduced into the co-sputtered film

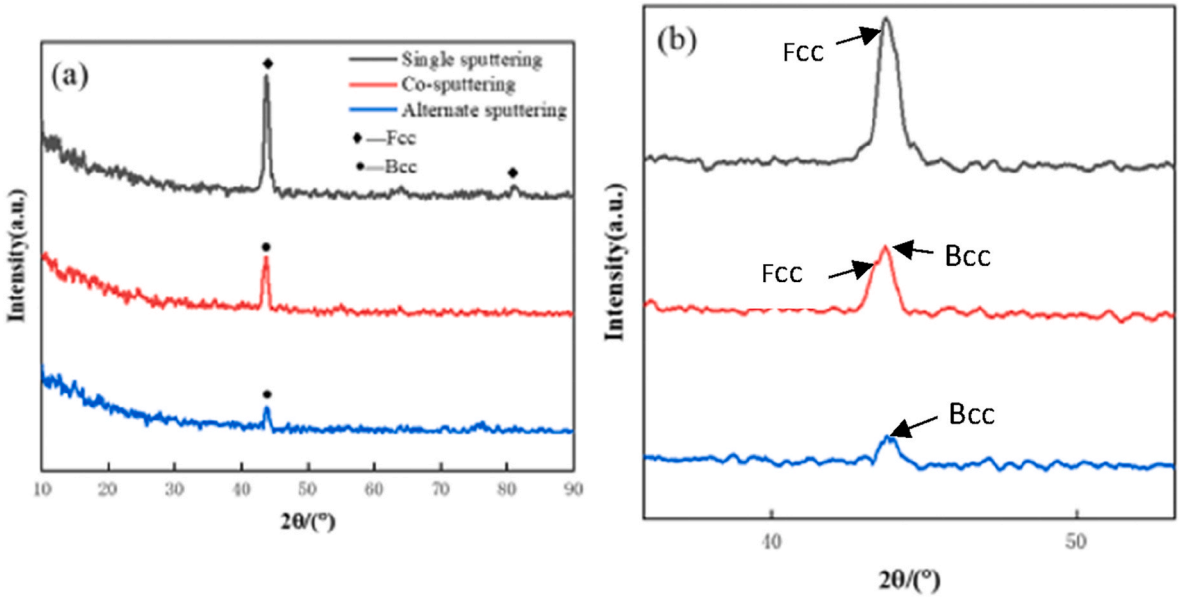

Fig. 1. (a) XRD patterns of the three FeCoNi(CuAl)$_{0.2}$ high entropy alloy films,(b) the detailed in the range of 2θ = 40–50°.

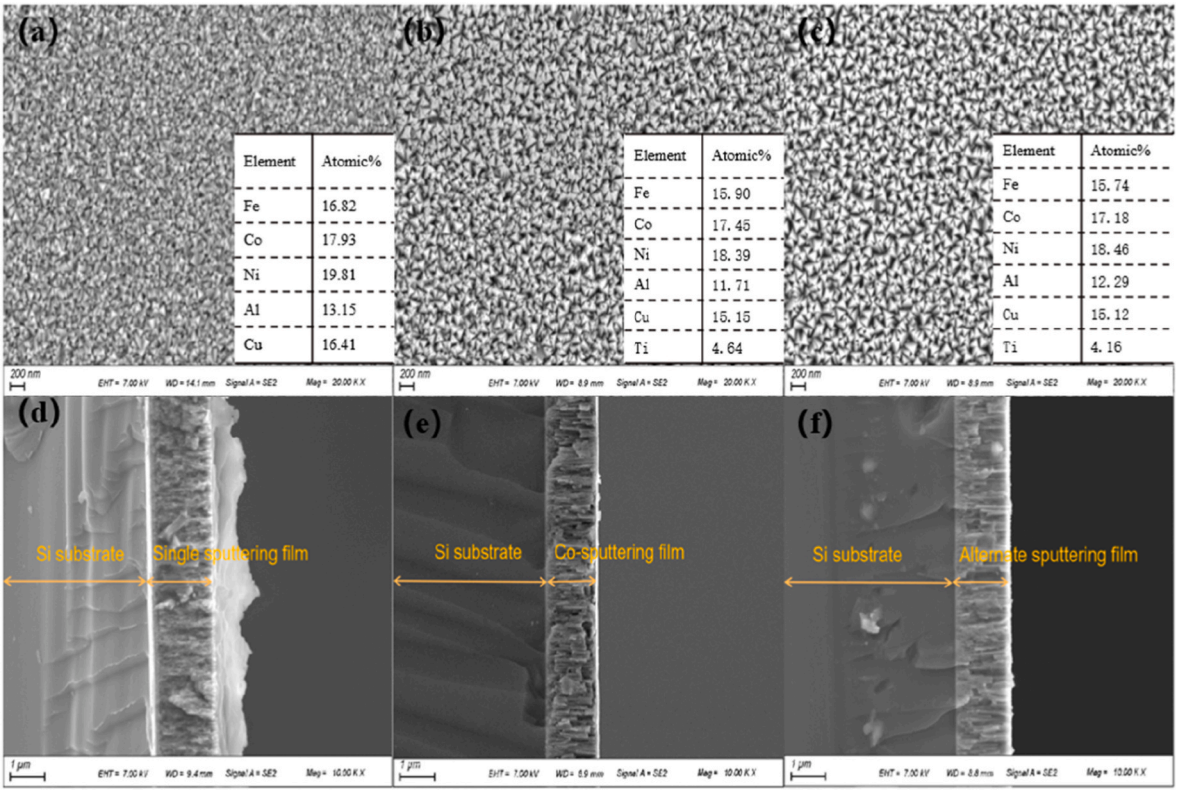

Fig. 2. SEM images with EDS data for FeCoNi(CuAl)$_{0.2}$ HEA films prepared using: (a) single sputtering; (b) co-sputtering; and (c) alternate sputtering techniques, with their respective morphologies (d–e).

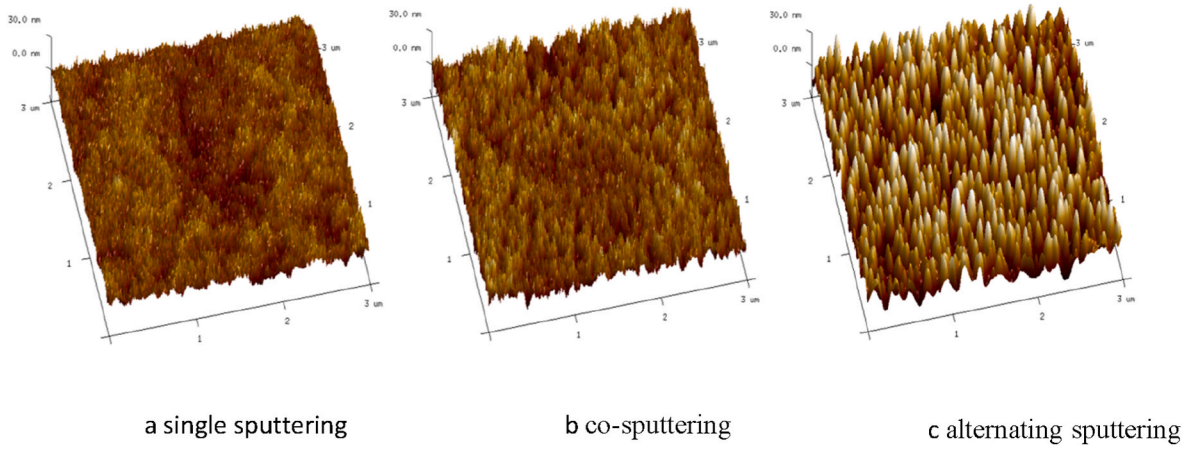

Fig. 3. AFM three-dimensional diagram of FeCoNi(CuAl)$_{0.2}$ high entropy alloy thin film.

Table 2
Roughness of FeCoNi(CuAl)$_{0.2}$ high entropy alloy thin film.

series	single sputtering film	co-sputtering film	alternating sputtering composite film
Ra/nm	3.59	4.79	8.67
Rq/nm	4.5	5.92	10.6
R_{max}/nm	37.5	50.9	76.9

and alternate sputtered FeCoNi(CuAl)$_{0.2}$ film system, the crystal properties of the films also varied. Specifically, the FCC structure changed to BCC, which is similar to that of Fe–Cr solid solution (PDF#34–0396). In a non-equimolar high entropy alloy system,the valence electron concentration VEC is helpful to understand and analyze the BCC or FCC structure. The calculation formula is as follows: $VEC = \sum_{i=1}^{n} Xi(VEC)_i$, Where, X_i is the mole fraction of component i in the alloy. According to the calculation, the VEC of FeCoNi(CuAl)$_{0.2}$ and FeCoNi(CuAl)$_{0.2}$Ti system are 8.56 and 6.42, respectively [1,10]. Therefore,Ti inhibits the formation of the FCC phase, and promotes the development of the BCC phase. For this reason, lattice distortion in the alloy coating intensifies, transforming the FCC phase into BCC.

Fig. 2 shows SEM images of the three films prepared with different sputtering schemes. As displayed in Fig. 2(a–c), the main elements of the FeCoNi(CuAl)$_{0.2}$ alloy (Fe, Co, Ni, Al, Cu, and Ti) were uniformly distributed in the sputtered films. Alloy mixing entropy was calculated according to Ref. [6] using the formula $\Delta S_{mix} = -R\sum_{i=1}^{n}(c_i \ln c_i)$, where c_i is the molar content of the ith component and R(8.314J-1 K·mol-1) is the gas constant. Results indicated that $\Delta Smix$ x for the HEA FeCoNi(CuAl)$_{0.2}$ studied in the present investigation was −11.73 kJ/mol, which is much higher than the entropy of binary intermetallic compounds. The high entropy of the system increased the compatibility of various elements and inhibited the formation of binary intermetallic compounds. Thus, single FCC or BCC structures were produced. EDS (Fig. 2d-f) was carried out taking as reference a line that included the substrate, homogeneous interface, and the sputtered films. Data indicated that thin films obtained by sputtering showed the presence of columnar crystals with a thickness of about 1 μm. In addition, uniform film thickness was observed, with no noticeable gap between the high entropy alloy thin films and the matrix. It was also observed that grain radial size decreased as sputtering modes changed.

Fig. 3 shows AFM three-dimensional diagram of FeCoNi(CuAl)$_{0.2}$ high entropy alloy thin film. In the single sputtering film, the surface has a fold shape, and the film layer is relatively uniform. In the cosputtering film, a small number of irregular shape pits begin to appear with the increase of Ti content, while a small agglomeration particles appear on the surface of the film, and the roughness increases slightly. In alternating sputtering films, the surface forms a relatively regular column-like crystal structure, so the roughness rises sharply. The average roughness (Ra), mean square roughness (Rq) and maximum roughness (Rmax) results are shown in Table 2.

Fig. 4 presents the results for hardness, modulus value, load, and indenting depth of different samples tested through nano-indentation experiments. Data showed that, when Ti content increased, the hardness of the three films gradually increased. Specifically, when single sputtering and co-sputtering were used, hardness presented values of 6.09 GPa and 7.33 GPa, respectively. In addition, Young's modulus also increased from 140 to 145 in the same order. This data can be further

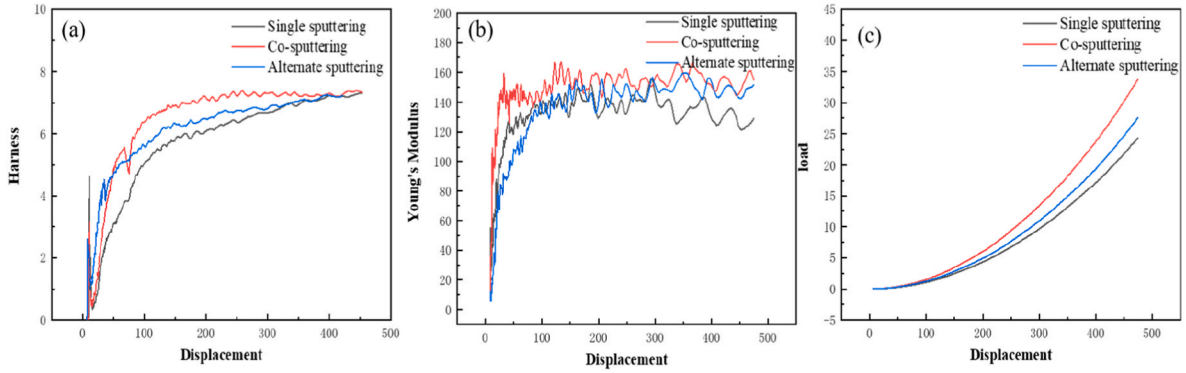

Fig. 4. Mechanical properties of FeCoNi(CuAl)$_{0.2}$ high entropy alloy films: (a) displacement-hardness curves; (b) displacement-Young's modulus; and (c) Displacement-load.

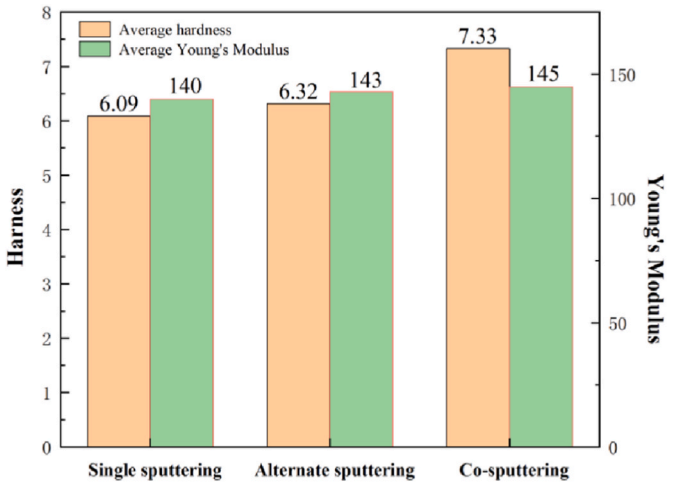

Fig. 5. Hardness and Young's modulus of FeCoNi(CuAl)$_{0.2}$ high entropy alloy films.

verified in Fig. 5, where variations in average hardness of the three films are presented.

Improvement in mechanical properties of high entropy alloy films can be attributed to the following factors: (1) The introduction of Ti lead to changes in phase structure and solution strengthening. The BCC structure formed by co-sputtering was more uniform than that obtained by alternate sputtering. In addition, BCC phase hardness was higher than that observed in the FCC structure, which was formed by single sputtering. With the increase in Ti content, film crystallinity decreased and the phase structure of the alloy changed, resulting in grain refinement. The high strength and hardness of co-sputtered films were obtained by strengthening the Al solution [1]; (2) Ti is an element with large atomic radius. This metal was solubilized into FeCoNi(CuAl)$_{0.2}$ by means of co-sputtering, increasing the difference in the atomic radius of the system. This parameter is represented as (δ) [7] and is calculated through $\delta = \sqrt{\sum_{i=1}^{n} c_i \left(1 - r_i \Big/ \left(\sum_{i=1}^{n} c_i r_i\right)\right)^2}$, where, r_i is the atomic radius of the ith component. Our calculations showed that atomic radius difference of single sputtering FeCoNi(CuAl)$_{0.2}$ films was $\delta_1 = 3.3\%$. However, after co-sputtering, $\delta_2 = 6.73\%$. The degree of lattice distortion is closely related to the type of selected alloying elements. Some studies have shown that the lattice distortion in the FeCoNiCr alloy system is almost negligible. However, with the increase in Pd content, lattice distortion becomes significant [8]. The introduction of Ti in the FeCoNi(CuAl)$_{0.2}$ system resulted in the intensification of lattice distortion. At the same time, the increase of atomic radius difference in the FeCoNi(CuAl)$_{0.2}$ system satisfies the critical shear strain γth spontaneously caused by lattice distortion. In addition, a strong functional relationship between the residual shear strain of "distorted lattice" and atomic radius difference was observed. Therefore, it can be concluded that Ti plays the same role in FeCoNi(CuAl)$_{0.2}$ as Pd in FeCoNiCr HEAs [6]. However, according to the results of Figs. 4 and 3, there is no direct correlation or influence between the hardness value of the film and its surface roughness.

4. Conclusions

Three types of FeCoNi(CuAl)$_{0.2}$ high entropy alloy films were prepared using different sputtering processes. The introduction of Ti reduced the crystallinity of the alloy and caused changes in the phase structure from FCC to BCC. The FeCoNi(CuAl)$_{0.2}$/Ti high entropy alloy films prepared by co-sputtering displayed excellent hardness and outstanding elastic modulus. Hardness and modulus values were 7.33 Gpa and 145 GPa, respectively. These results indicated that the Ti solution with large atomic radius caused significant lattice distortion and solution strengthening.

CRediT authorship contribution statement

J.N. Wen: Writing – original draft. **R.J. Wu:** Writing – original draft. **Y.H. Mi:** Investigation. **N. Zhang:** Investigation. **Z.H. Lin:** Investigation. **S.C. chen:** Experiment, Characterization. **Y.Q. Li:** Experiment, Characterization. **S.F. Yang:** Writing – review & editing.

Declaration of competing interest

The authors declare that they have no known competing financial interests or personal relationships that could have appeared to influence the work reported in this paper.

Data availability

No data was used for the research described in the article.

Acknowledgments

This study was supported by the Major Innovation project of Nanjing Institute of Technology(CKJA202102), Open Fund of Jiangsu Provincial Key Laboratory of Advanced Structural Materials and Applied Technology(ASMA202107), Jiangsu University Student Innovation and Entrepreneurship Program(202111276035Y), and Postgraduate Research & Practice Innovation Program of Jiangsu Province(SJCX21-0934).

References

[1] J.W. Yeh, S.K. Chen, S.J. Lin, et al., J. Adv. Mater. 6 (2004) 299–303.
[2] X. F Wang, Y. Zhang, Y. Qiao, G. L Chen, Intermetallics (15) (2007) 357–362.
[3] T.Y. Ma, M. Yan, K.Y. Wu, et al., Acta Mater. 142 (2018) 18–28.
[4] S. Shuang, Z. Yding, D. Chung, et al., Corrosion Sci. 164 (2020), 108315.
[5] A. Mazilkin, B.B. Straumal, S.G. Protasova, et al., 199 (2021): 109417.
[6] Q.Q. Ding, Y. Zhang, X. Chen, et al., Nature 574 (2019) 223–227.
[7] T.Y. Ma, M. Yan, K.Y. Wu, et al., Acta Mater. 142 (2018) 18–28.
[8] Y. Yang, Q.F. He, Acta Metall. Sin. 57 (2021) 385–392.
[9] M.H. Liu, H.Q. Li, J. Wang, et al., Materials (2008) 4–7, 08.
[10] J. Piotr, J. Dariusz M, L. Zhang, et al., Mater. Des. (2022) 216.
[11] S. Alvi, D.M. Jarzabek, M.G. Kohan, et al., ACS Appl. Mater. Interfaces 12 (18) (2020).